

## Wavelet Cleaning of Solar Dynamic Radio Spectrograms

Robert A. Sych<sup>1,2</sup> \* and Yi-Hua Yan<sup>1</sup>

<sup>1</sup> National Astronomical Observatories, Chinese Academy of Sciences, Beijing 100012

<sup>2</sup> Institute of Solar-Terrestrial Physics, Russian Academy of Sciences, Irkutsk 664033, Russia

Received 2001 December 11; accepted 2001 December 25

**Abstract** By applying the state-of-the-art mathematical apparatus, the wavelet transformation, we explore the possibility of a dynamic cleaning of raw data obtained with the Chinese solar radio spectrographs over a wide wavelength range (from 0.7 to 7.6 GHz). We consider the problem of eliminating the interference caused by combination rates of data sampling (10–20 ms), and the low-frequency interference (4–30 s) caused by the receiving equipment changing its characteristics with time. It is shown that the best choice to reconstruct a signal suffering from amplitude, frequency and phase instabilities, is by means of wavelet transformation at both high and low frequencies. We analysed observational data which contained interferences of nonsolar origin such as instrumental effects and other man-made signals. A subsequent comparison of the reference data obtained with the acousto-optical receiver of the Siberian Solar Radio Telescope (SSRT) with the “cleaned” spectra confirms the correctness of this approach.

**Key words:** Sun: radio radiation — methods: data analysis

### 1 INTRODUCTION

When analyzing time series having the periodic structure of internal harmonics with time-varying amplitude-phase characteristics, there often arises a difficulty of filtering the meaningful signal from resulting noise. In the search for periodicities of time series and their subsequent filtering, it is customary to use Fourier-transform (FT). Fourier-coefficients that are obtained as a result of the transform, are amenable to sufficiently simple interpretation. However, the application of spectral analysis based on Fourier-transform has one disadvantage, namely, FT works poorly in cases where the parameters of the process vary in time (unsteady character), and since it gives averaged coefficients for the entire time series under investigation remote events make an equal contribution along with recent events. In other words, FT affords good resolution in frequency but poor resolution in time. Therefore, FT is effective only when processing periodic signals. Formal application of direct and inverse Fourier-transform to such signals as solar radio emission can give rise to various artifacts, false periodicities, etc. This is

---

\* E-mail: [sych@iszf.irk.ru](mailto:sych@iszf.irk.ru)

caused both by the signal behavior itself (non-periodicity) and by the sudden character of most of the signal, which does not permit the signal to be correctly reconstructed.

Aperiodic time series are characteristic for many receivers with real, rather than ideal time behavior. The main contribution in the shaping of the waveform is from the instrumental function of the receiver (in our case, the receiver of the solar wideband radio spectrometer). As a consequence of the fact that the amplitude-frequency characteristics of the receiver channels differ from each other, the signals we acquire at the receiver output have varying amplitudes, frequencies and phases. It should also be noted that these signal characteristics have a tendency to change in time. A convolution of the instrumental function with the real signal from the Sun leads to an integrated signal, the form of which will depend strongly on the state of the receiver equipment. Accordingly, it is necessary to try to filter out the harmonics introduced by the equipment.

As pointed out above, noise harmonics represent an aperiodic component of the signal with a complicated interaction of the amplitude, frequency and phase variation. Therefore, to use standard Fourier-transform for the filtering will be unsuitable. A way to resolve this issue is to apply wavelet transform (WT) (Grossmann et al. 1984; Daubechies 1988, 1990, 1991; Farge 1992), in which the signal under consideration is compared not with an infinite sinusoid (as is done in Fourier-transform) but with a finite wave train. An instructive practical implementation of wavelet transform provides the possibility of reconstructing the real signal through the filtering of certain frequencies. It does not give multiple harmonics and is effective for investigating the spectral properties of aperiodic signals (Holschneider 1995).

## 2 THE MAIN CHARACTERISTICS OF SOLAR BROADBAND DYNAMIC RADIO SPECTROMETER

We will consider an example of the data obtained at Huairou station - solar dynamic radio spectra. Each spectrum represents a set of time scans of the radio signal from the Sun at selected frequencies. The data used in the present analyses were observed by the newly developed Solar Radio Broadband Fast Dynamic Spectrometers located at the Huairou Solar Observing Station, Beijing Astronomical Observatory (BAO). The whole system covers five frequency bands: 0.7–1.4 GHz, 1.0–2.0 GHz, 2.6–3.8 GHz, 4.5–7.5 GHz (intensity only), and 5.2–7.6 GHz for both polarization and intensity observations with high temporal and frequency resolutions (Fu et al. 1995). The performance of three of the spectrometers is shown in Table 1 and they were put into operation in 1994 January, 1996 September, and 1999 August, respectively. The solar radio telescopes were moved to Huairou in 1999, and the radio environment has been measured and analyzed to ensure the reliability of the observations and data reduction (Yan et al. 2001a, 2001b).

**Table 1** Solar Radio Spectrometers at Huairou of NAOC

Frequency range (GHz)	Spectral resolution (MHz)	Time resolution (ms)	Sensitivity ( $S_0^*$ )	Dynamic range (dB)	Polarizations	Start Working
1.0 – 2.0	20	100	2%	10	Yes	1994
2.6 – 3.8	10	8	2%	10	Yes	1996
5.2 – 7.6	20	5	2%	10	Yes	1999

\* where “ $S_0$ ” denotes solar radio flux from quiet Sun.

### 3 THE WAVELET-TRANSFORM AS A BANDPASS FILTER

Wavelet-transform represents a relatively new direction in the family of spectral analyzers and implies expanding the time series in terms of the basis formed by a special family of wavelet functions. The wavelets constitute a set of oscillating self-similar functions of different scales which are localized in both the physical and Fourier spaces. These functions have a zero mean and a sufficiently fast decrease at infinity. Unlike traditional one-dimensional Fourier-transform, i.e., expansion in terms of frequencies, one-dimensional wavelet-transform ensures a two-dimensional expansion of the one-dimensional signal under investigation. Furthermore, the frequency and coordinate are regarded as independent variables. In the case of Fourier-transform where the basis is represented by a set of functions obtained from a basic function, the sinusoid, by varying the frequency, a family of wavelets is also produced from a certain basic function through time shifts and scale changes. Continuous Fourier-transform is performed through a convolution of the function  $f(t)$  that is analyzed with a two-parametric wavelet function  $\psi_{a,b}$  (Astaf'eva 1996), and each of wavelet function  $\psi_{a,b}$  of a given family is obtained from its "parent" function  $\psi$  through extension-contraction and shift

$$\psi_{ab}(t) = |a|^{-1/2} \psi\left(\frac{t-b}{a}\right), \quad (1)$$

where the parameter  $a$  is the wavelet width and  $b$  the shift parameter. Thus all wavelet functions of a given family are self-similar and have a constant number of oscillations.

Integral wavelet transform  $(W_\psi f)(a, b)$  of the function  $f(t)$  is

$$(W_\psi f)(a, b) = |a|^{-1/2} \int_{-\infty}^{+\infty} f(t) \overline{\psi\left(\frac{t-b}{a}\right)} dt = \int_{-\infty}^{+\infty} f(t) \overline{\psi_{ab}(t)} dt. \quad (2)$$

Moreover, the function  $\psi$  must satisfy the condition:

$$C_\psi = \int_{-\infty}^{+\infty} \frac{|\hat{\psi}(\omega)|^2}{|\omega|^{-1}} d\omega < \infty, \quad (3)$$

where  $\hat{\psi}(\omega)$  is the Fourier-transform of the function  $\psi(t)$ .

Formulas (2) and (3) may also be written in the Fourier-space

$$(W_\psi f)(a, b) = \int_{-\infty}^{+\infty} \overline{\hat{\psi}(a\omega)} f(\omega) e^{ib\omega} d\omega, \quad (4)$$

and

$$f(\omega) = C_\psi^{-1} \iint \hat{\psi}(a\omega) (W_\psi f) e^{-ib\omega} \frac{dadb}{a^2}. \quad (5)$$

Because wavelet-transform is a broadband filter with known response function (base wavelet), it is possible to reconstruct the signal using inverse transform as an inverse filter (Donoho 1994). This is suitable for orthogonal wavelet transform (which has an orthogonal basis); however, for continuous wavelet transform this is complicated because of the redundancy in space and time.

On the other hand, such a redundancy makes it possible to utilize different basic functions to reconstruct the time series (Daubechies 1988). In this case the series represents the sum of the real part of WT at all scales. With the basic parameters (a, b) there exists a formula of inverse wavelet transform

$$f(t) = C_{\psi}^{-1} \iint (W_{\psi} f)(a, b) \psi_{ab}(t) \frac{da db}{a^2}, \quad (6)$$

where  $C_{\Psi}$  represents a coefficient analogous to the  $(2\pi)^{1/2}$  in Fourier-transform

$$C_{\psi} = \int_{-\infty}^{\infty} |\hat{\psi}(\omega)|^2 |\omega|^{-1} d\omega < \infty. \quad (7)$$

As opposed to Fourier-transform, wavelet transform retains the locality of representation of the signal, which makes it possible to locally reconstruct the signal (Torrence et al. 1998). Also, there is a possibility of reconstructing a part of the signal or to single out the contribution of a certain scale. There is a connection between the local behavior of the signal and the local behavior of its wavelet-coefficients. Here, for obtaining a part of the reconstructed signal, it is necessary to consider the coefficients referring only to the corresponding subregion of the wavelet space. For instance, if the function  $f(x)$  is locally smooth, then the corresponding wavelet-coefficients remain small; if, however,  $f(x)$  contains a singularity such as a burst, then in its vicinity the amplitude of the wavelet-coefficients increases considerably. In the case where the wavelet-coefficients involve random errors, they will act on the reconstructed signal only near the position of the perturbation, whereas Fourier-transform extends these errors throughout the entire signal being reconstructed. Fourier-transform is also especially sensitive to phase errors as a consequence of the alternating character of trigonometric series, whereas such a situation does not occur in wavelet-transform. Furthermore, there is a possibility of correcting the errors that are present in the wavelet-coefficients of continuous transform, thanks to the redundancy inherent in continuous wavelet-transform, which provides a way of using this method to investigate time series with gaps in the data.

Since  $(W_{\psi} f)(a, b)$  contains combined information on the analyzing wavelet and the input signal, the selection of the analyzing wavelet determines what information should be extracted from the signal. Each wavelet has characteristic properties in the time and frequency spaces. Therefore, by using different wavelets it is possible to additionally reveal and stress some or other properties of the signal that is being analyzed. In the present case we have used a complex basis based on the Morlet's wavelet (Grossmann 1984) which is well localized in both the scale and frequency plane, and this makes it possible to rapidly reconstruct the signal even in the presence of a singularity such as short-lived bursts or in the absence of signal

$$\Psi_0 = \pi^{-1/4} e^{i\omega_0 \mu} e^{-\eta^2/2}, \quad (\text{Morlet's wavelet-function}) \quad (8)$$

and

$$\hat{\Psi}_0 = \Theta(\omega) \exp \left[ -\frac{(\omega - \omega_0)^2}{2} \right], \quad (\text{Fourier-transform of the Morlet's function}) \quad (9)$$

where  $\omega_0$  is the dimensionless frequency. With increasing  $\omega_0$ , there is an increase in angular selectivity of the basis, but the spatial selectivity is impaired. For that reason, we selected an optimum value, at which high (both angular and spatial) resolution is achieved.

#### 4 ANALYSIS AND DISCUSSION

A preliminary analysis of the signals from the radio spectrometers at different frequencies in the range 0.7–7.6 GHz showed that all noise present in the signals can be arbitrarily divided into two classes: high-frequency noise that is associated with the combination frequencies of data sampling, and low-frequency noise that is produced by changes of amplitude-frequency characteristics of the receiver with time. It should be noted that the power of combination frequencies is a variable quantity depending on which frequency channel the signal is recorded. Low-frequency noise, in turn, represents mainly multiple harmonics (4–30 s), which are phase-shifted and different in amplitude. For instance, the range 5.2–7.6 GHz comprises four subranges (5.2–5.8, 5.8–6.4, 6.4–7.0, and 7.0–7.6 GHz) which differ from each other by an abrupt phase change of the noise signal. Furthermore, the period also changes in a complicated wave-like fashion, leading to a drastic distortion of the real signal. The character of the noise behavior makes an unambiguous description in the time and frequency domains impossible. Therefore, the application of Fourier-transform for reconstructing the signal becomes unsuitable. The only method that is applicable for filtering is wavelet-transform, it provides a way to localize and eliminate the noise along both the time and frequency axes without introducing distortions into the real signal.

For the purpose of a practical implementation of the wavelet method, a software was developed using the algorithmic language IDL (Interactive Dialog Language) for examining solar dynamic spectra over a wide frequency range, carrying out their pre-treatment, including obtaining two-dimensional images in the L- and R-polarization channels, the intensity (L+R), circular polarization (L-R), and the degree of polarization, as well as keeping track of frequency drifts. Furthermore, examination of the different parts of the spectrum involved using dynamic temporal and frequency corrections with the possibility of calibrating, from the integral flux, the unperturbed part of the spectrum. The wavelet cleaning of dynamic spectra uses a program unit for reconstructing useful signals with the possibility of expanding the frequency range of the wavelet spectrum to cover all the frequencies present in the spectra.

With the knowledge of the frequency range of the noise harmonics, we can approximate it, upon constructing the wavelet spectrum for one frequency of the dynamic radio spectrum, to the entire signal reception band. By cutting out the noise frequency range of the wavelet spectrum and reconstructing the signal from the resulting expansion coefficients for each of the receiver's frequencies, we obtain real signals, which, ultimately, provide us with a "pure" dynamic radio spectrum. In this case the two-dimensional amplitude spectrum (frequency/period-time) provides a possibility of identifying the noise components and keeping track of their behavior in time. For acquiring the information of different frequency ranges where large differences in the amplitude of expansion coefficients were observed, the logarithmic scale was used.

We tested the possibilities of cleaning the high-frequency component using wavelet-transform with the observational data of 2001 March 30. On that day, at Huairou Station the solar radio dynamic spectrometer (SRDS) recorded a powerful burst with a series of strongly polarized subsecond-duration pulses (SSP) in the range 5.2–7.6 GHz. This burst was also recorded with the acousto-optical receiver of SSRT in the range 5675.24–5786.69 MHz, and the record was used as a reference for temporal and spatial referencing of the two observations (Fig. 1). Data sampling was 5 ms for the SRDS and 14 ms for the AOR SSRT. The burst was produced by the active region NOAA 9393 which during its solar disk passage was characterized by high geomagnetic activity.

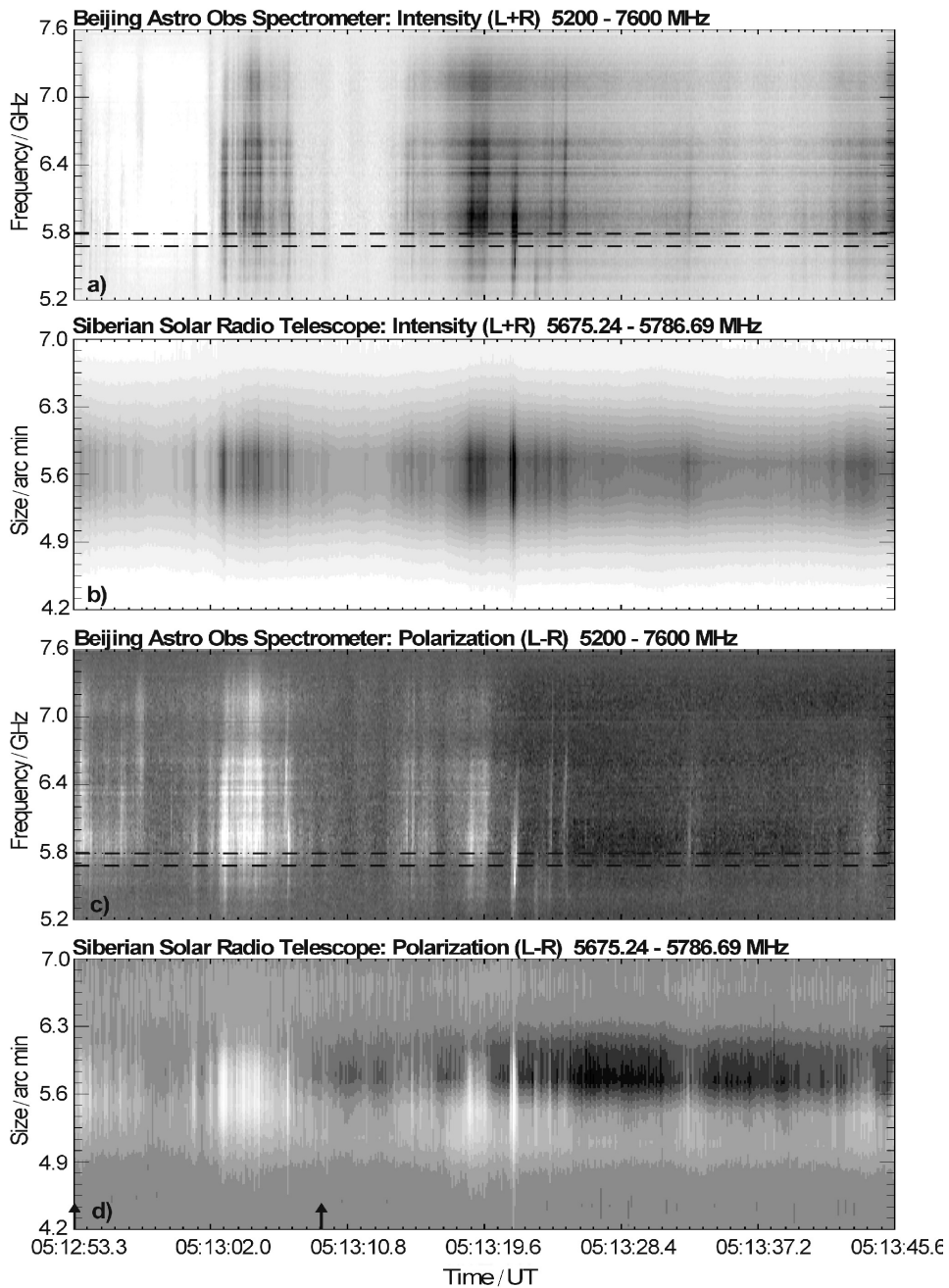


Fig. 1 Radio burst with a series of subsecond pulses on 2001 March 30. Figures 1 (a, c) are the dynamic radio spectra in the range 5.2–7.6 GHz with a time resolution of 5 ms. Broken lines show the SSRT working band. Figures 1 (b, d) are the time sweeps of 1-D scanning of the radio source NOAA 9393 in which the burst occurred. The source was 2.8 min of arc in size and the time resolution was 14 ms. All the images are displayed both in the intensity (L+R) and circular polarization (L–R) channels. The arrows indicate the interval of wavelet cleaning.

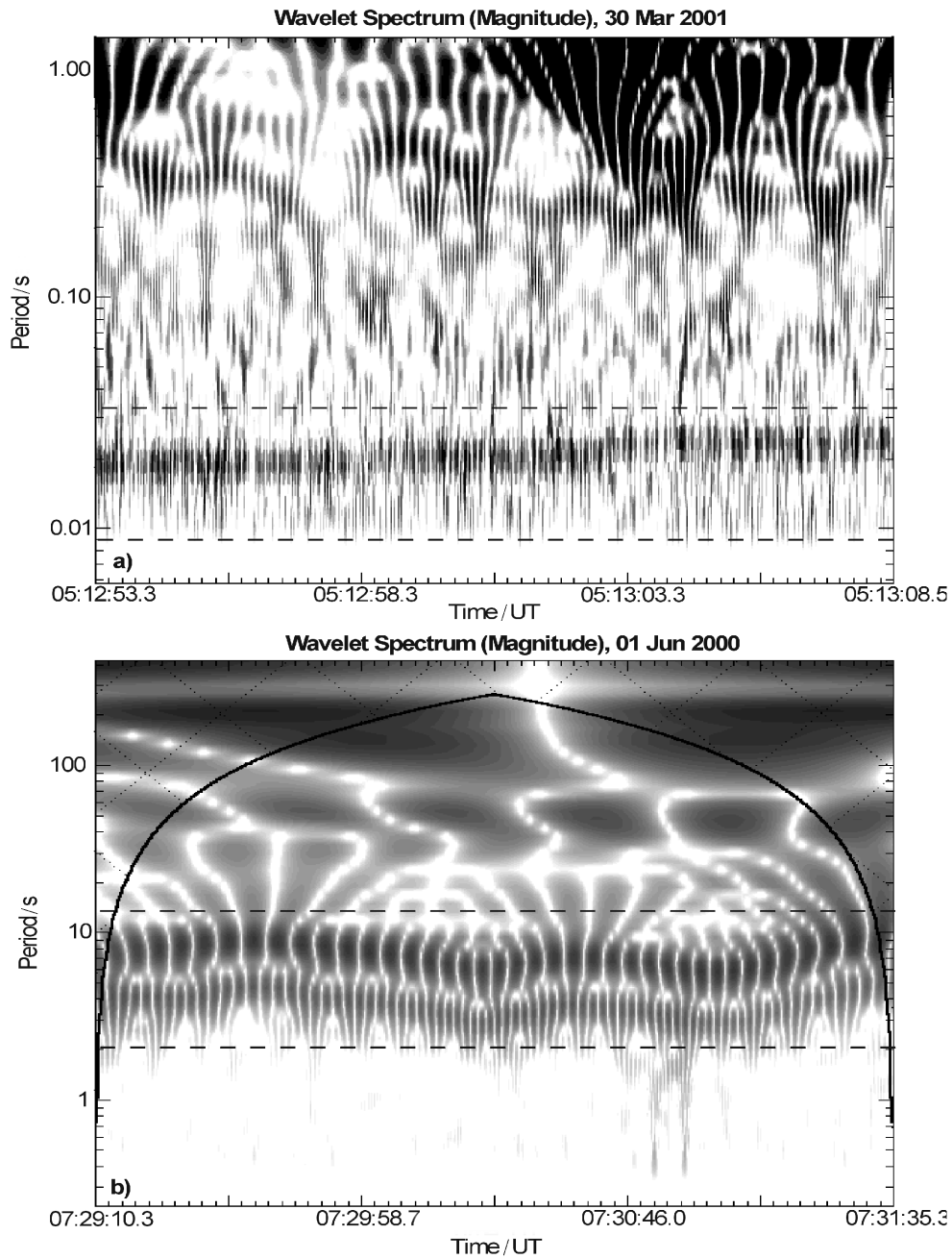


Fig. 2 Amplitude wavelet spectrum for two radio bursts: 2001 March 30 (a), and 2000 June 1 (b). The period and expansion coefficients are given on a logarithmic scale. Broken lines indicate the interval of the noise components that were removed. The reliability interval of the frequencies identified is indicated by the dome-shaped curve.

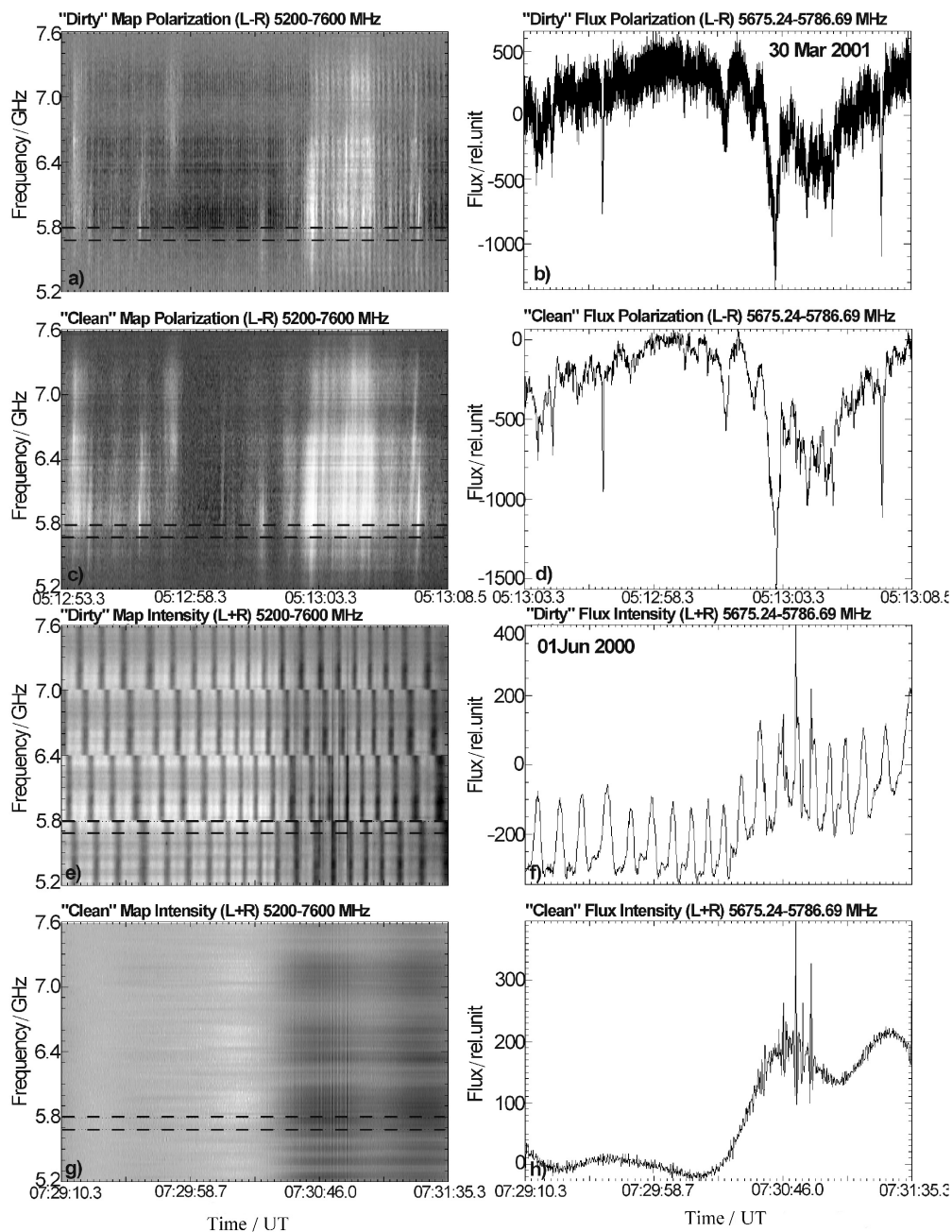


Fig. 3 Example of wavelet cleaning of solar dynamic radio spectra in the range 5.2–7.6 GHz. Left: maps of spectra prior to and after the cleaning on two dates, 2001 March 30 (polarization channel (L-R), high-frequency noise Fig. 3a, c), and 2000 June 01 (intensity channel (L+R), low-frequency noise, Fig. 3e, g). Right: time profiles of the integral radio flux in the SSRT frequency range (shown by broken lines) for the corresponding dates prior to and after the wavelet cleaning.

Figure 1 (a–d) shows the dynamic spectra of the solar radio emission burst in the intensity and circular polarization channels in the range 5.2–7.6 GHz (Fig. 1a, c) as well as the time profiles of the local source NOAA 9393 in the additive operation mode of the SSRT (Fig. 1b, d). The start time of the identified portion of the burst is 05:12:53.26 UT, and the duration is 52.7 s. It can be seen that there is a one-to-one correspondence between the brightness variations in the dynamic spectra and in the radio source, both for fast processes such as subsecond pulses and for the background component.

For comparing the spectra prior to and after wavelet cleaning, we use the portion of the burst indicated by the two arrows in Fig. 1. Figure 3 (a, b) shows this portion of the burst and its integral spectrum in the working band of the SSRT (5675.24–5786.69 MHz). It is evident that there exists a periodicity in the form of a noise component. This is confirmed by the constructed amplitude wavelet spectrum for the mean frequency of the SSRT’s working band (Fig. 2a). The figure clearly shows narrow bands of harmonics of about 10–20 ms which represent combined frequencies caused by the sampling of data from the radio spectrometer. By cutting out these harmonics and reconstructing the signal from the remaining spectral components, we obtain a “pure” radio spectrum (Fig. 3c, d). In this case all fast components such as subsecond pulses are totally retained in the dynamic radio spectrum.

In a similar way, we determined the capability of wavelet cleaning in regard to lower-frequency components. Figure 3 (e) shows the dynamic radio spectrum of the 2000 June 01 burst in the preflare stage of its development, which was characterized by broadband short-lived pulses present in the time structure. Fig. 3 (f) gives the integral flux variation in the SSRT range. Noises with different amplitudes, frequencies and phases were observed. By applying wavelet transform, we obtain a two-dimensional amplitude spectrum showing two clearly observed multiple harmonics at 4 and 8 s (Fig. 2b). Upon removing them and reconstructing the signal throughout the entire band of the radio spectrum, we obtain a “pure” spectrum (Fig. 3g, h). This image of the dynamic spectrum shows that the cleaning has been done correctly.

To determine the reliability of the dynamic radio spectra that have been subjected to the wavelet cleaning procedure, the radio flux variation for the spectrometer in the SSRT band was compared with the reference flux of the local source in which the burst occurred. Space and time characteristics were acquired with the acousto-optical receiver of the SSRT with records taken at 14 ms interval. A cross-correlation analysis showed that the time shift between the data from the Beijing radio spectrometer and the SSRT is 28 ms, which appears to be an error of data measurement. The coefficient of linear correlation is 0.98. All the results confirm the validity of the solution for the problem formulated and show that the application of wavelet-transform (direct and inverse) is the best way for cleaning dynamic radio spectra with complicated characters in the received signals.

**Acknowledgements** This work was supported by the Russian Foundation for Basic Research (Nos. 00-02-16819, 00-15-96710, 01-02-16290), and by Federal program “Astronomy”. This work was also supported by the Chinese Academy of Sciences, the NSFC (19833050, 19973008) and the Ministry of Science and Technology of China (G2000078403).

**References**

- Astaf'eva N. M., 1996, *Uspekhi Fizicheskikh Nauk*, 166, 11
- Daubechies I., 1988, *Comm. Pure Appl. Math.*, 41, 906
- Daubechies I., 1990, *IEEE Trans. Inform. Theory*, 36, 961
- Daubechies I., 1991, *Ten Lectures on Wavelets (CBMS Lecture Notes Series)*, Philadelphia: SIAM
- Donoho D. L., Johnstone I. M., 1994, *Biometrika*, 81, 3
- Farge M., 1992, *Ann. Rev. Fluid. Mech.*, 24, 395
- Fu Q., Qin Z., Ji H. et al., 1995, *Solar Phys.*, 160, 97
- Grossmann A., Morlet J., 1984, *SIAM, J. Math. Anal.*, 15, 723
- Holschneider M., 1995, *Wavelets: An Analysis Tool*, Oxford: Oxford Univers. Press, p.455
- Torrence C., Compo G. P., 1998, *Bull. Amer. Meteo. Soc.*, 79, 1
- Yan Y., Fu Q., Liu Y. et al., 2001a, R. J. Cohen, W. T. Sullivan, III, eds., *Preserving the Astronomical Sky*, IAU Symp., No. 196, p.311
- Yan Y., Ji H., Fu Q. et al., 2001b, R. J. Cohen, W. T. Sullivan, III, eds., *Preserving the Astronomical Sky*, IAU Symp., No. 196, p.315